

Effects of meson-exchange currents on the $(\vec{\epsilon}, e'p)$ structure functions

V. Van der Sluys, J. Ryckebusch, and M. Waroquier

Institute for Theoretical Physics and Institute for Nuclear Physics, Proeftuinstraat 86, B-9000 Gent, Belgium

(Received 28 September 1993)

The response functions for the unpolarized $(e, e'p)$ and polarized $(\vec{\epsilon}, e'p)$ reaction are calculated for medium-heavy nuclei under quasifree conditions. The formalism presented here incorporates both electron distortion effects and two-body currents related to meson-exchange and the $\Delta(1232)$ excitation. The final-state interaction of the outgoing nucleon with the residual nucleus is handled in a self-consistent Hartree-Fock random phase approximation formalism. The effect of Coulomb distortion of the incoming and outgoing electron is included within a fully distorted wave calculation. The sensitivity of the results to the two-body currents is discussed for the five structure functions in quasielastic $(\vec{\epsilon}, e'p)$ scattering off the target nuclei ^{16}O and ^{40}Ca . A selective sensitivity to the two-body currents is obtained in the longitudinal-transverse interference term W_{LT} for which two-body currents can explain part of the discrepancy between the impulse-approximation calculations and the data.

PACS number(s): 21.60.Jz, 24.10.Eq, 25.30.Fj

I. INTRODUCTION

The coincidence $(e, e'p)$ reaction when performed under quasifree conditions has proven to be an excellent tool in the study of single-particle properties of the nucleus [1]. The analysis of the quasielastic $(e, e'p)$ reaction yields information on the single-particle wave functions, spectroscopic factors, and strength distributions. Generally, the quasielastic $(e, e'p)$ results have been analyzed within the framework of a relativistic [2,3] or nonrelativistic [4–6] distorted wave impulse approximation (DWIA) approach. In these models the quasielastic electromagnetic response is assumed to be dominated by one-body currents. Hence, the nuclear current is handled in the impulse approximation (IA) in which it will be regarded as the sum of the one-body currents from the individual nucleons. The final-state interaction of the outgoing proton with the residual nucleus is treated in a distorted wave

approximation either within an optical potential model [4] or within a microscopic Hartree-Fock random phase approximation (HF-RPA) approach [7,8]. In most cases, the quasielastic $(e, e'p)$ cross sections are reasonably well reproduced within this DWIA approach.

At present, improved experimental techniques have become available and measurements have been carried out to extract more detailed information on the response to the longitudinal and transverse polarization states of the virtual photon. Assuming the one-photon exchange approximation, the unpolarized $(e, e'p)$ cross section can be written in terms of four nuclear structure functions each multiplied with a different kinematical factor. In case of polarized incoming electrons, an additional helicity $h(\pm 1)$ dependent structure function W'_{LT} can be extracted [9,10]. The angular distribution of the polarized $(\vec{\epsilon}, e'p)$ cross section is determined by the following expression:

$$\frac{d^3\sigma}{dE_f d\Omega_{E_f} d\Omega_{p_p}}(\vec{\epsilon}, e'p) = C \{v_L W_L + v_T W_T + v_{TT} W_{TT} \cos 2\varphi_p + v_{LT} W_{LT} \cos \varphi_p + h v'_{LT} W'_{LT} \sin \varphi_p\}. \quad (1)$$

All five structure functions W depend on the momentum and energy transfer (\mathbf{q}, ω) of the virtual photon, the proton momentum p_p , and proton angle θ_p . The angle between the scattering plane and the reaction plane is denoted by φ_p . The convention for the different scattering angles is fixed in Fig. 1. The various structure functions W are independent of the electron kinematics and are sensitive in a particular way to a different aspect of the reaction mechanism. A complete experimental determination of the structure functions W , under suitable electron kinematics, could yield additional information on the reaction mechanism and might impose a constraint on the available theoretical models. Determination of all five structure functions demands polarized electrons and out-of-plane experiments which are generally difficult to realize.

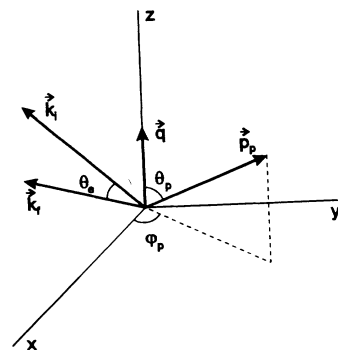


FIG. 1. Conventions for the scattering angles in the $(e, e'p)$ reaction.

Recently, new results of in-plane measurements have become available for $^{16}\text{O}(e, e'p)$ [11–13] and $^{40}\text{Ca}(e, e'p)$ [13,14]. These experiments yield information on three nuclear structure functions $W_L + (q^2/2q_\mu q^\mu)W_{TT}$, W_T , and W_{LT} . In Ref. [11] the $^{16}\text{O}(e, e'p)$ data have been compared with the results of the nonrelativistic and relativistic DWIA calculations of Van Orden *et al.* Both theoretical models are found to produce comparable results pointing towards relativity playing a rather unimportant role in quasielastic kinematics. Both DWIA results succeed in reproducing separately the shapes of the total cross section and structure functions. However, a serious inconsistency appears since the fitted reduction factors for the $^{16}\text{O}(e, e'p)^{15}\text{N}(1/2^-, \text{g.s.})$ and the $^{16}\text{O}(e, e'p)^{15}\text{N}(3/2^-, 6.32 \text{ MeV})$ cross sections largely deviate from those for the corresponding W_{LT} terms. Other $(e, e'p)$ separation measurements on ^{16}O and ^{40}Ca have been performed at NIKHEF-K [12,13]. These data have been confronted with the nonrelativistic DWIA model of the Pavia group [4]. For the $(e, e'p)$ processes feeding the residual $(A-1)$ nucleus in its ground state ($1p_{1/2}$ knockout in ^{16}O and $1d_{3/2}$ knockout in ^{40}Ca) a fair agreement between theory and the separated response functions is observed. For knockout from the corresponding spin-orbit partners ($1p_{3/2}$ in ^{16}O and $1d_{5/2}$ in ^{40}Ca) the absolute W_{LT} is considerably larger than what the theory predicts. This observation suggests that the quasielastic electron excitation of the nucleus is more complex than it was generally believed.

The aim of the present work is to go beyond the DWIA by including two-body contributions in the nuclear current from meson-exchange and intermediate delta excitations and to investigate the effect of these two-body currents on the structure functions. Second, the effect of higher-order diagrams, such as electron distortion, is investigated and the sensitivity of the cross section and structure functions to these distortions is discussed. The organization of this paper is as follows. In Sec. II we give an outline of the theoretical model we adopt. Section III contains a discussion of the effect of electron distortion and two-body components in the nuclear current on the cross sections and structure functions for $^{16}\text{O}(e, e'p)$ and $^{40}\text{Ca}(e, e'p)$. The calculations are compared with data from NIKHEF-K and Saclay. Finally, some conclusions are drawn.

II. FORMALISM

A. Two-body currents

In order to determine the structure functions in expression (1), the following transition matrix elements of the nuclear current

$$\langle J_R M_R; \mathbf{p}_p, \frac{1}{2} m_{s_p} | J_\mu(q) | J_i M_i \rangle \quad (2)$$

have to be calculated. The final state in this matrix element refers to the residual nucleus in a state $| J_R M_R \rangle$ and an escaping proton with momentum \mathbf{p}_p and spin projection m_{s_p} . Throughout this work the residual nucleus is considered to remain in a pure hole state relative to the ground state $| J_i M_i \rangle$ of the target nucleus. The spectroscopic factor, extracted from a least squares fit of the calculated cross section to the data, reflects the amount of hole strength in the final state. The wave function for the escaping particle and the residual nucleus is obtained in the continuum RPA formalism as described in Ref. [7]. The RPA formalism involves a multipole expansion of the final state $| J_R M_R; \mathbf{p}_p, 1/2 m_{s_p} \rangle$ in terms of linear combinations of particle-hole and hole-particle excitations out of a correlated ground state. As such we account for the multistep processes of the type depicted in Fig. 2(a). Bound and continuum single-particle states are taken to be eigenstates of the HF mean-field potential obtained with an effective interaction of the Skyrme type (SKE2) [15]. In this way, we naturally preserve the orthogonality between the bound and the continuum states.

In the present approach, the nuclear current in the matrix element of Eq. (2) is taken to be the sum of a one-body and a two-body operator. The nucleonic one-body term consists of the well-known convection and magnetization current. The two-body current is taken from a nonrelativistic reduction (retaining only terms up to the order $1/M^2$ in the nucleon mass) of the lowest-order Feynman diagrams with one exchanged pion and intermediate delta excitation. We assume pseudovector coupling of the pion to the nucleon. This procedure gives rise to the seagull terms [Fig. 2(b)], the pion-in-flight term [Fig. 2(c)], and terms with a $\Delta(1232)$ excitation in the intermediate state [Fig. 2(d)]. In this nonrelativistic approach the nuclear charge operator is not affected by two-body contributions. In the static limit, the two-body current related to the diagrams of Fig. 2 reads in momentum space as [16]

$$\mathbf{J}^{(2)}(\mathbf{q}; \mathbf{q}_1 \mathbf{q}_2) = \mathbf{J}_{\text{seag}}^{(2)}(\mathbf{q}; \mathbf{q}_1 \mathbf{q}_2) + \mathbf{J}_{\text{pion}}^{(2)}(\mathbf{q}; \mathbf{q}_1 \mathbf{q}_2) + \mathbf{J}_{\text{delta}}^{(2)}(\mathbf{q}; \mathbf{q}_1 \mathbf{q}_2), \quad (3)$$

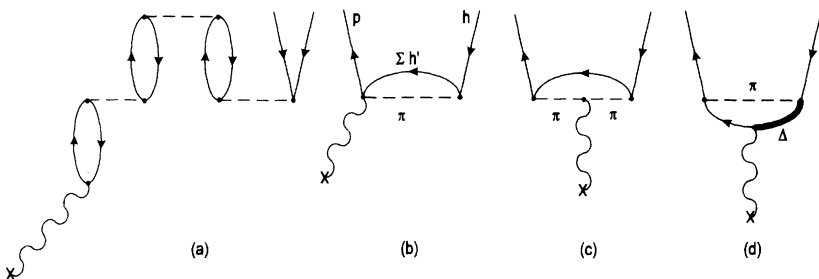


FIG. 2. Diagrams for the $(e, e'p)$ reaction. Diagrams of the type (a) imply virtual photon absorption on a single nucleon. Diagrams of the type (b) (seagull term), (c) (pion-in-flight term) and (d) (intermediate Δ creation) refer to absorption on a two-body operator.

with

$$\mathbf{J}_{\text{seag}}^{(2)}(\mathbf{q}; \mathbf{q}_1 \mathbf{q}_2) = -ie \left(\frac{f_{\pi NN}}{m_\pi} \right)^2 F_{\gamma N}(q) (\boldsymbol{\tau}_1 \times \boldsymbol{\tau}_2)^3 \left\{ \frac{\boldsymbol{\sigma}_1(\boldsymbol{\sigma}_2 \cdot \mathbf{q}_2)}{\mathbf{q}_2^2 + m_\pi^2} - \frac{\boldsymbol{\sigma}_2(\boldsymbol{\sigma}_1 \cdot \mathbf{q}_1)}{\mathbf{q}_1^2 + m_\pi^2} \right\},$$

$$\mathbf{J}_{\text{pion}}^{(2)}(\mathbf{q}; \mathbf{q}_1 \mathbf{q}_2) = ie \left(\frac{f_{\pi NN}}{m_\pi} \right)^2 F_{\gamma\pi}(q) (\boldsymbol{\tau}_1 \times \boldsymbol{\tau}_2)^3 \frac{(\boldsymbol{\sigma}_1 \cdot \mathbf{q}_1)(\boldsymbol{\sigma}_2 \cdot \mathbf{q}_2)}{(\mathbf{q}_1^2 + m_\pi^2)(\mathbf{q}_2^2 + m_\pi^2)} (\mathbf{q}_1 - \mathbf{q}_2),$$

$$\mathbf{J}_{\text{delta}}^{(2)}(\mathbf{q}; \mathbf{q}_1 \mathbf{q}_2) = i \frac{2f_{\gamma N\Delta} f_{\pi N\Delta} f_{\pi NN}}{9m_\pi^3(m_\Delta - m_N)} F_{\gamma\Delta}(q) \left\{ 4 \frac{(\boldsymbol{\sigma}_2 \cdot \mathbf{q}_2)}{\mathbf{q}_2^2 + m_\pi^2} \mathbf{q}_2 \tau_2^3 - (\boldsymbol{\tau}_1 \times \boldsymbol{\tau}_2)^3 \left(\frac{\boldsymbol{\sigma}_2 \cdot \mathbf{q}_2}{\mathbf{q}_2^2 + m_\pi^2} (\boldsymbol{\sigma}_1 \times \mathbf{q}_2) \right) + 1 \leftrightarrow 2 \right\} \times \mathbf{q}.$$

In these expressions the following coupling constants are adopted: $\frac{f_{\pi NN}^2}{4\pi} = 0.079$, $\frac{f_{\pi N\Delta}^2}{4\pi} = 0.37$ and $f_{\gamma N\Delta}^2 = 0.014$.

To account for the composite structure of the γN , $\gamma\pi$, and $\gamma\Delta$ vertices, electromagnetic form factors have to be introduced. For the γN form factor ($F_{\gamma N}$) we use the common dipole form [17]. Current conservation with the one-pion exchange potential is merely satisfied for the seagull and the pion-in-flight current in case that the pion ($F_{\gamma\pi}$) and nucleon ($F_{\gamma N}$) form factor coincide. In all further calculations we have adopted the $F_{\gamma\pi}$ extracted from the vector dominance model [18]. The delta current is divergenceless and can be multiplied with an arbitrary form factor without violating the charge-current conservation rules. For simplicity, we assumed that $F_{\gamma\Delta} = F_{\gamma N}$ in all calculations presented here. The short-range structure of the πNN and $\pi N\Delta$ vertices is implemented in a phenomenological way by introducing hadronic form factors. As is usually done the monopole form is adopted. For both types of vertices the same pion cutoff mass Λ_π ($= \Lambda_{\pi NN} = \Lambda_{\pi N\Delta}$) is used.

The final-state wave function in the matrix element of Eq. (2) is evaluated using a multipole expansion in

terms of distorted waves. The nuclear current operator is decomposed in the well-known electric and magnetic transition operators T_{JM}^{el} and T_{JM}^{mag} [7,19]. If we restrict ourselves to doubly closed-shell nuclei ($J_i = 0$) and to the evaluation of the diagrams depicted in Fig. 2, reduced matrix elements of the following type

$$\langle 0^+ || T_J^{(1)}(q) + T_J^{(2)}(q) || ph^{-1}(J; \omega) \rangle \quad (4)$$

remain to be calculated. In this expression $T_J^{(1)}$ and $T_J^{(2)}$ refer to the IA and the pionic contribution. The residual nucleus is considered to remain in a pure hole state h relative to the ground state of the target nucleus. The single-particle (s.p.) state p denotes a continuum state with energy $\epsilon_p = \omega - |\epsilon_h| > 0$. The two-body part of the transition operators is handled exactly and involves two active nucleons in the absorption process (Fig. 2). Hence, in the evaluation of Eq. (4), this two-body part has been expressed in terms of two-body matrix elements in the following way:

$$\begin{aligned} \langle 0^+ || T_J^{(2)}(q) || ph^{-1}(J; \omega) \rangle &= \sum_{h' J_1 J_2} \sqrt{2J_1 + 1} \sqrt{2J_2 + 1} (-1)^{j_h - j_{h'} - J - J_2} \left\{ \begin{matrix} j_h & j_{h'} & J_1 \\ J_2 & J & j \end{matrix} \right\} \\ &\times \langle (hh') J_1 || T_J^{(2)}(q) || (ph'); J_2 \rangle_{\text{as}}. \end{aligned} \quad (5)$$

The sum runs over all occupied proton and neutron s.p. states h' . The explicit expression for the antisymmetrized two-body matrix elements for the diagrams of Fig. 2 can be found in Ref. [20].

B. Electron distortion

In the previous sections the $(\vec{e}, e'p)$ reaction was handled assuming the one-photon exchange approximation. As a correction to this first-order approach we have accounted for higher-order diagrams due to electron distortion, i.e., the initial and final electrons are allowed to

scatter elastically from the nucleus. These corrections are governed by the full charge distribution of the nucleus and consequently are of the order of $Z\alpha$. The effect of electron distortion, due to the static Coulomb field generated by the nucleus, is treated to all orders in a Coulomb distorted wave born approximation (CDWBA). We have taken the initial and final electron wave functions to be solutions of the electron Dirac equation in a central Coulomb field $V(r)$ generated by a homogeneous spherical charge distribution, and to satisfy the outgoing (+) and incoming (-) boundary conditions. The electron wave functions are obtained with a phase shift analysis based on a partial wave expansion, i.e.,

$$\bar{\Psi}_{\mathbf{k}, m_s}^{E(\pm)}(\mathbf{r}, \sigma) = \frac{1}{\sqrt{2}(2\pi)^{\frac{3}{2}}} \sum_{j,l} \sum_{m_l, m} 4\pi i^l e^{\pm i\delta_{lj}^E} \langle l m_l \frac{1}{2} m_s | j m \rangle Y_{l m_l}^*(\Omega_{\mathbf{k}}) (\bar{l} - l) \begin{pmatrix} \frac{G_{lj}^E(r)}{r} \varphi_{l \frac{1}{2}}^{j m}(\Omega_r, \sigma) \\ i \frac{F_{lj}^E(r)}{r} \varphi_{l \frac{1}{2}}^{j m}(\Omega_r, \sigma) \end{pmatrix}. \quad (6)$$

The initial or final electron is completely characterized by its energy E , momentum \mathbf{k} , and spin polarization m_s . The functions $G_{lj}^E(r)$ and $F_{lj}^E(r)$ are solutions of the radial Dirac equation which has to be solved numerically for each partial wave. In the ultrarelativistic limit, they satisfy the following relations:

$$G_{lj}^E(r) = (\bar{l} - l) F_{lj}^E(r), \quad (7)$$

$$G_{lj}^E(r) \xrightarrow{r \rightarrow \infty} (\bar{l} - l) \frac{\sin[kr - \eta \ln(2kr) - \frac{l\pi}{2} + \delta_{lj}^E]}{k}. \quad (8)$$

In these expressions \bar{l} stands for $j + 1/2$ ($j - 1/2$) for $l = j - 1/2$ ($j + 1/2$). The phase shift caused by the Coulomb potential $V(r)$ is denoted by δ_{lj}^E .

In CDWBA, the expression for the $(\vec{e}, e'p)$ cross section becomes rather involved due to the double partial wave expansion of the outgoing proton wave function and the distorted electron waves. On top of that, the numerical evaluation of the cross sections is getting complicated due to the large amount of electron partial waves we have to take into account due to the long-range character of

the Coulomb interaction. The limit $Z \rightarrow 0$ (equivalent with neglecting the electron distortions) can be considered as a severe test of the accuracy of the numerical techniques employed in CDWBA. Our code has been checked to obey this requirement. In this particular case the electron wave function (6) reduces to a plane wave and the DWBA cross section of Eq. (1) should be retained. Details regarding the adopted numerical procedure will be reported elsewhere [21]. For a more elaborate theoretical discussion of electron distortion we refer the reader to Refs. [21–23].

When considering electron distortion, the electron and nuclear transition part in the $(\vec{e}, e'p)$ cross section can no longer be separated. Consequently, the simple plane wave form of the cross section (1) as a function of five nuclear structure functions each multiplied with a kinematical factor does no longer hold. Experimentally, however, the structure functions are extracted from the $(\vec{e}, e'p)$ cross section assuming the DWBA. The charge-current interference structure function W_{LT} is obtained from the asymmetry in the measured cross section as a function of missing momentum $p_m = \pm |\mathbf{p}_p - \mathbf{q}|$:

$$W_{LT}(p_m) = \frac{1}{2v_{LT}C} \left\{ \frac{d^3\sigma}{dE_f d\Omega_{E_f} d\Omega_{p_p}}(p_m) - \frac{d^3\sigma}{dE_f d\Omega_{E_f} d\Omega_{p_p}}(-p_m) \right\}. \quad (9)$$

Under the conventions of Fig. 1, p_m is positive for $\varphi_p = 0^\circ$ and negative for $\varphi_p = 180^\circ$. Although the function W_{LT} does not separate along the lines of Eq. (1) when Coulomb distortion is taken into account, theoretically, it can be evaluated according to Eq. (9). This means that the calculations precisely match what is measured. The main difference with the DWBA is the dependence of the distorted structure function on the kinematical variables such as electron energies and electron scattering angles.

III. RESULTS AND DISCUSSION

All results presented here are obtained under the kinematical conditions of the $^{16}\text{O}(e, e'p)$ [12,13] and $^{40}\text{Ca}(e, e'p)$ [13,14] NIKHEF-K experiments and the $^{16}\text{O}(e, e'p)$ experiment of Chinitz *et al.* [11]. All these experiments were performed under perpendicular kinematics, respectively, at $(\omega, \mathbf{q}) = (96 \text{ MeV}, 460 \text{ MeV})$ (^{16}O), $(116 \text{ MeV}, 446 \text{ MeV})$ (^{40}Ca), and $(172 \text{ MeV}, 570 \text{ MeV})$ (^{16}O). Hereafter, the different kinematical conditions will be referred to as kinematics I, II, and III. The cross sections and structure functions are plotted as a function of the missing momentum p_m . The ^{40}Ca data are presented in terms of the reduced cross section ρ_m extracted from the cross section in the following way:

$$\rho_m(p_m) = \frac{1}{p_p E_p \sigma^{cc1}} \frac{d^3\sigma}{dE_f d\Omega_{E_f} d\Omega_{p_p}}(p_m). \quad (10)$$

The differential cross section is divided by the electron-proton cross section σ^{cc1} as defined by DeForest [24]. In the plane wave impulse approximation this reduced cross section $\rho_m(p_m)$ is related to the probability of finding a bound proton in the target nucleus in a given shell with momentum p_m .

In order to get a feeling for the size of electron distortion effects in the considered $(e, e'p)$ reactions, the (reduced) cross sections and W_{LT} response for $^{16}\text{O}(e, e'p)^{15}\text{N}(1p_{1/2}^{-1})$, $^{16}\text{O}(e, e'p)^{15}\text{N}(1p_{3/2}^{-1})$, $^{40}\text{Ca}(e, e'p)^{39}\text{K}(1d_{3/2}^{-1})$, and $^{40}\text{Ca}(e, e'p)^{39}\text{K}(1d_{5/2}^{-1})$ have been calculated in DWIA and CDWIA (Figs. 3 and 4). The final-state interaction of the escaping proton with the residual nucleus is accounted for within the RPA approach using the one-body current [Fig. 2(a)]. Although the importance of two-body contributions in the nuclear current will be established in the next paragraphs, we omitted them in these calculations for numerical reasons. Given the fact that we are dealing with relatively light target nuclei, it is apparent that the effect of electron distortion on the cross sections is relatively small. In fact, the separated structure functions are more sensitive

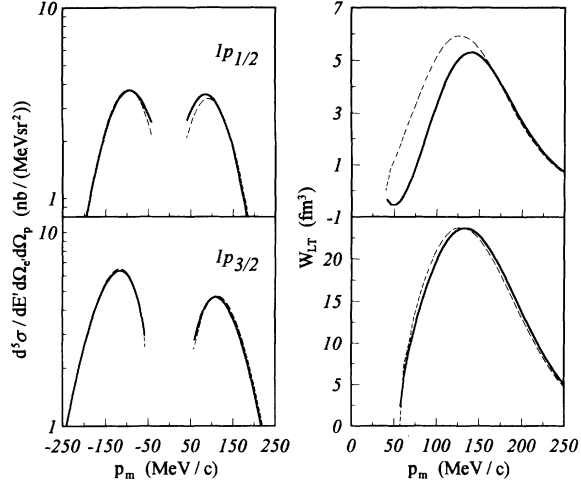


FIG. 3. The cross sections and the W_{LT} response for $^{16}\text{O}(e, e'p)^{15}\text{N}(1p_{1/2}^{-1})$ and $^{16}\text{O}(e, e'p)^{15}\text{N}(1p_{3/2}^{-1})$ (kinematics I). The full and dashed lines were computed, respectively, within CDWIA and DWIA. No spectroscopic factors are considered.

to the distortion effects than the total cross section. In the forthcoming discussion it will become clear that the modification of the interference structure function W_{LT} due to electron distortion effects takes smaller proportions than the modification related to two-body currents. Since the calculation of the electron distortion effects in combination with two-body currents is numerically hard to realize, the effect of two-body currents has been studied in a DWBA framework.

Some theoretical uncertainties exist with respect to the pion cutoff mass Λ_π in the hadronic form factor and to the electromagnetic pion form factor. Before confronting our theoretical approach with the data, we investigate the sensitivity of the results to these parameters. Whereas parametrization of nucleon-nucleon scattering

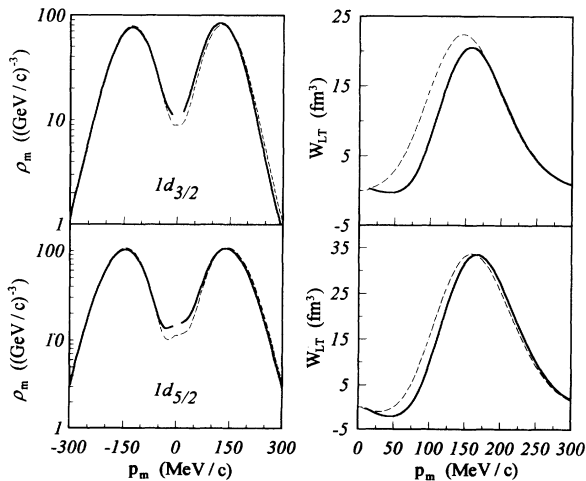


FIG. 4. The reduced cross sections and the W_{LT} response for $^{40}\text{Ca}(e, e'p)^{39}\text{K}(1d_{3/2}^{-1})$ and $^{40}\text{Ca}(e, e'p)^{39}\text{K}(1d_{5/2}^{-1})$ (kinematics II). Same line conventions as in Fig. 3. No spectroscopic factors are included.

data in terms of the Bonn potential leads to a cutoff mass $\Lambda_\pi = 1200$ MeV [25], recent studies on the triton system [26] seem to prefer a smaller value ($\Lambda_\pi = 810$ MeV). We have performed calculations including all diagrams depicted in Fig. 2 with different values of Λ_π . As a representative example we display in Fig. 5(a) the longitudinal-transverse interference structure function W_{LT} for proton knockout out of the $1p_{3/2}$ orbit in $^{16}\text{O}(e, e'p)$ under the kinematics I. Results are displayed for a pion cutoff mass that should be considered as a lower limit ($\Lambda_\pi = 650$ MeV) and an upper limit ($\Lambda_\pi = 1200$ MeV). Also shown is the W_{LT} structure function as obtained within the IA. The uncertainty of the results due to the theoretical ambiguity in Λ_π should be estimated around 20% of the total two-body contribution. In all further calculations we used a cutoff mass $\Lambda_\pi = 800$ MeV. This cutoff mass, which is smaller than the one obtained in the Bonn potential, is believed to account for heavier mesons in an effective way [16].

The sensitivity of the present approach to the $F_{\gamma\pi}$ form factor in the pion-in-flight current is investigated in Fig. 5(b). We have plotted the transverse structure function W_T for proton knockout out of the $1p_{3/2}$ orbit in ^{16}O under kinematics I. The results including the full nuclear current are compared with the IA predictions. Two different $F_{\gamma\pi}$ form factors are considered in the calculations. First, the pion form factor is set equal to the nucleon form factor and, as a consequence, current conservation is satisfied. Second, we adopt the $F_{\gamma\pi}$ form factor as derived from the vector dominance model.

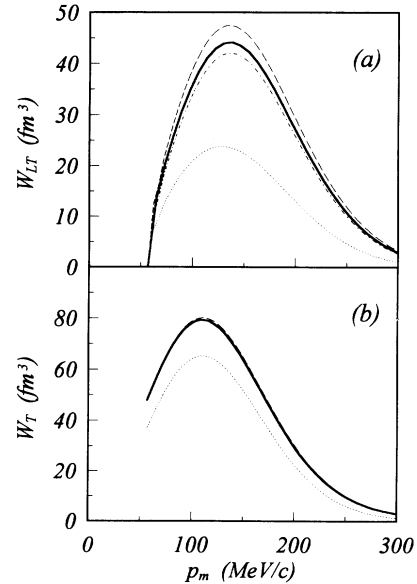


FIG. 5. Structure functions for $^{16}\text{O}(e, e'p)$ from the $1p_{3/2}$ orbit including one (dotted line) and two-body contributions in the nuclear current. (a) W_{LT} for different values of the pion cutoff mass in the hadronic form factor. Dash-dotted line: $\Lambda_\pi = 650$ MeV; dashed line: $\Lambda_\pi = 1200$ MeV; full line: $\Lambda_\pi = 800$ MeV. (b) W_T considering different expressions for the pion form factor. Dashed line: $F_{\gamma\pi} = F_{\gamma N}$; full line: $F_{\gamma\pi}$ from vector dominance model. No spectroscopic factors are considered.

Clearly, the results are rather insensitive to the choice of the pion form factor.

The impact of the different components in the nuclear current on the cross sections and structure functions in the $^{16}\text{O}(e, e'p)$ reaction is illustrated in Figs. 6–10. For each of the two considered kinematical conditions, the calculated cross section and corresponding structure functions are multiplied with *one and the same* spectroscopic factor. This spectroscopic factor is extracted from a best fit to the data of the calculated cross section considering the full nuclear current (including one- and two-body terms). The same reduction factor is adopted for all intermediate results. In Figs. 6 and 7 we display the cross sections and corresponding longitudinal, transverse, and interference structure functions $W_L + (q^2/2q_\mu q^\mu)W_{TT}$, W_T , and W_{LT} for $^{16}\text{O}(e, e'p)^{15}\text{N}(1p_{1/2}^{-1}, \text{g.s.})$ and $^{16}\text{O}(e, e'p)^{15}\text{N}(1p_{3/2}^{-1}, 6.32 \text{ MeV})$ under kinematics I. Even in the IA, the longitudinal and transverse structure functions are reasonably well described. As for in-plane experiments the longitudinal structure function cannot be separated from the cross section, the minor modification of this structure function due to two-body currents can be ascribed to the contribution of the transverse-transverse structure function W_{TT} . In confor-

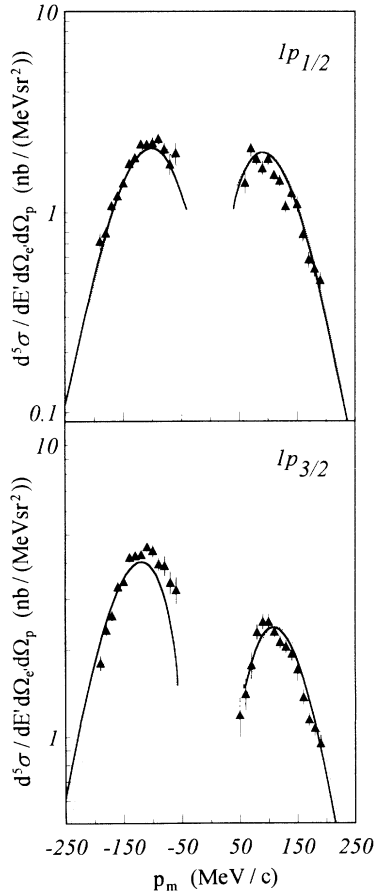


FIG. 6. Cross sections for proton knockout off ^{16}O from the $1p_{1/2}$ and $1p_{3/2}$ orbit including one- (dotted line) and two-body contributions (full line) in the nuclear current. The data are from Ref. [12]. All curves are multiplied with a spectroscopic factor [$S(1p_{1/2}) = 0.60$, $S(1p_{3/2}) = 0.51$].

mity with the results of Refs. [4,13] we do not arrive at a *simultaneous* description of the total cross section and the W_{LT} structure function in the IA. Furthermore, a spin-orbit dependence of the results is observed: Whereas the IA seems to work reasonably well for the $1p_{1/2}$ state, the absolute value of W_{LT} is severely underestimated for the $1p_{3/2}$ orbit. This mismatch in W_{LT} between experiment and the IA is also reflected in a bad theoretical description of the asymmetry in the measured cross section. For both s.p. states the seagull and pion-in-flight current exhibit the same characteristics. This general behavior is illustrated in Fig. 8 on the basis of the interference structure function W_{LT} for the $1p_{1/2}$ and $1p_{3/2}$ orbits. Whereas the seagull contribution enhances the transverse and charge-current interference response functions, the pion-in-flight current has the opposite effect. Generally, the pion-in-flight term has a smaller influence on the structure functions than the seagull current. The spin-dependent behavior of the W_{LT} term for the two states originates from the contribution of the $\Delta(1232)$ current. For the $1p_{1/2}$ state a further quenching is observed in contrast with the $1p_{3/2}$ results where the devi-

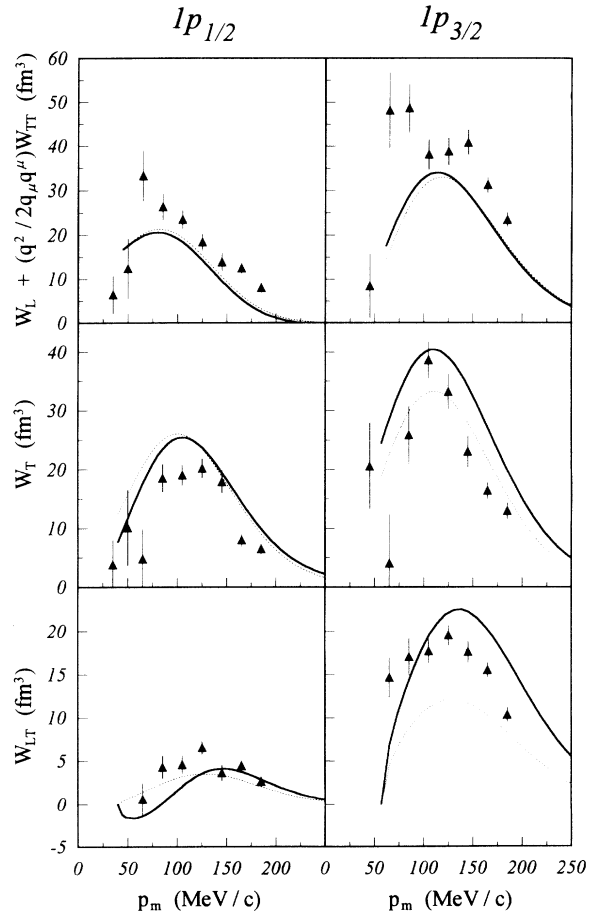


FIG. 7. Structure functions $W_L + q^2/(2q_\mu q^\mu)W_{TT}$, W_T , and W_{LT} for proton knockout off ^{16}O from the $1p_{1/2}$ and $1p_{3/2}$ orbit including one- (dotted line) and two-body contributions in the nuclear current. For the full line all diagrams of Fig. 2 were accounted for. The data are from Ref. [12]. The curves are multiplied with the same spectroscopic factors as in Fig. 6.

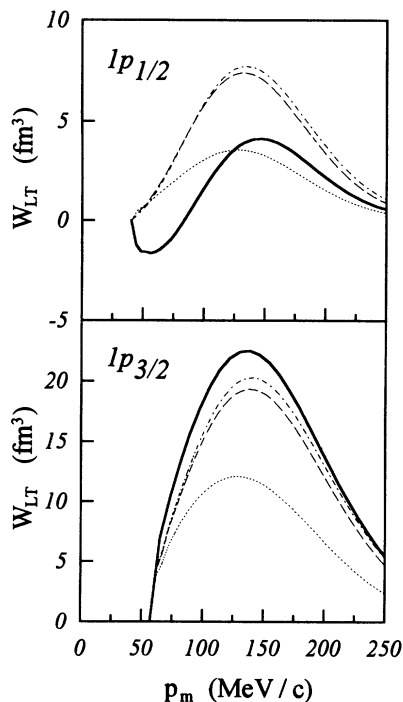


FIG. 8. Structure function W_{LT} for proton knockout off ^{16}O from the $1p_{1/2}$ and $1p_{3/2}$ orbit. Dotted line: one-body current, dash-dotted line: one-body and seagull currents, dashed line: one-body, seagull, and pion-in-flight currents. For the full line the full current is considered. The curves are multiplied with the same spectroscopic factors as in Fig. 6.

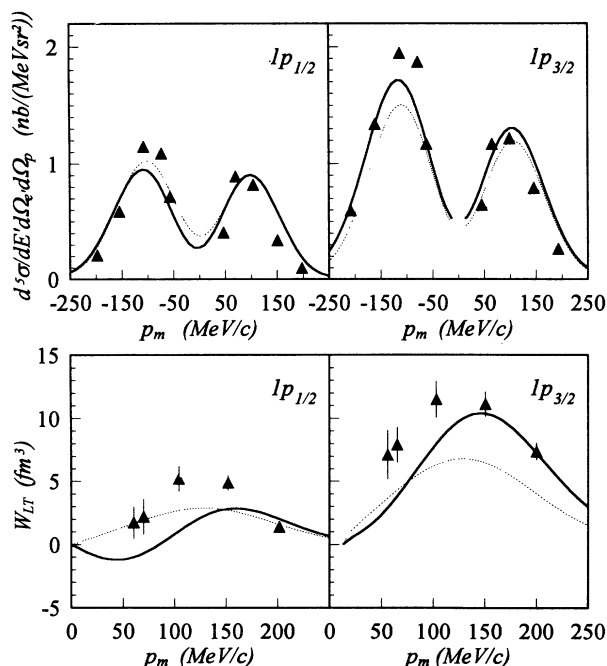


FIG. 9. Cross sections and interference structure functions W_{LT} for $^{16}\text{O}(e, e'p)$ from the $1p_{1/2}$ and $1p_{3/2}$ orbits including one- (dotted line) and two-body contributions (full line) in the nuclear current. The data are from Ref. [11]. The curves are multiplied with the following spectroscopic factors $[S(1p_{1/2}) = 0.49, S(1p_{3/2}) = 0.41]$.

ation from the IA approach becomes more pronounced. As can be noticed, the discrepancy between the measured W_{LT} and the DWIA results for the $1p_{3/2}$ state can be partially ascribed to the two-body contributions in the nuclear current. In contrast to the cross section for which the effect of the pionic currents is hardly visible, two-body contributions in the nuclear current cannot be discarded in order to obtain a complete description of the separated structure functions.

In order to underline the general character of the previous conclusions, we carried out a second calculation for $^{16}\text{O}(e, e'p)$ at slightly different kinematics (III) (Fig. 9). Again, cross sections and structure functions show a similar behavior as before with respect to the meson contributions in the current. Moreover, the discrepancy between the data and the predictions in the IA are partially cleared up. However, an unresolved problem remains. Whereas we would expect that in both kinematics the same spectroscopic factors should be obtained, the Saclay data $[S(1p_{1/2}) = 0.49$ and $S(1p_{3/2}) = 0.41]$ produce values that are about 20% smaller than those obtained from the NIKHEF-K measurements $[S(1p_{1/2}) = 0.60$ and $S(1p_{3/2}) = 0.51]$. Other groups have also pointed out this problem [12]. Spaltro *et al.* [12] compared CDWIA calculations of the Pavia group for both kinematics and found two different sets of spectroscopic factors.

In Fig. 10 we display the fifth structure function W'_{LT} as can be extracted from the polarized $^{16}\text{O}(\vec{e}, e'p)$ reaction for the same orbits. To our knowledge, no data of this response function are available as yet. In the near future, polarization experiments will be carried out at MIT-Bates [27]. From a theoretical standpoint, this ad-

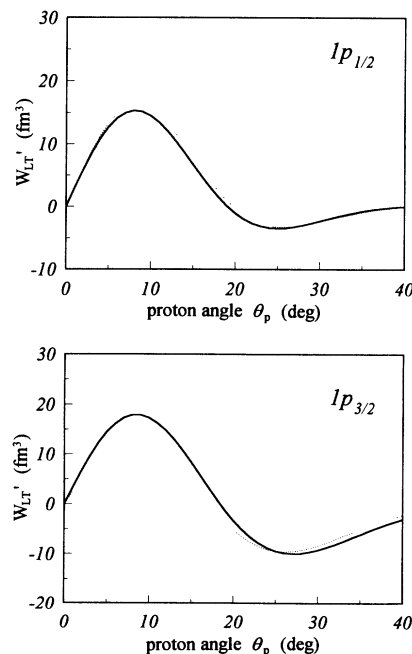


FIG. 10. W'_{LT} for the $(\vec{e}, e'p)$ reaction off ^{16}O from the $1p_{1/2}$ and $1p_{3/2}$ orbit under the kinematics I including (a) only one-body contributions in the nuclear current (dotted line) and (b) both one- and two-body contributions in the nuclear current (full line). No spectroscopic factors are included.

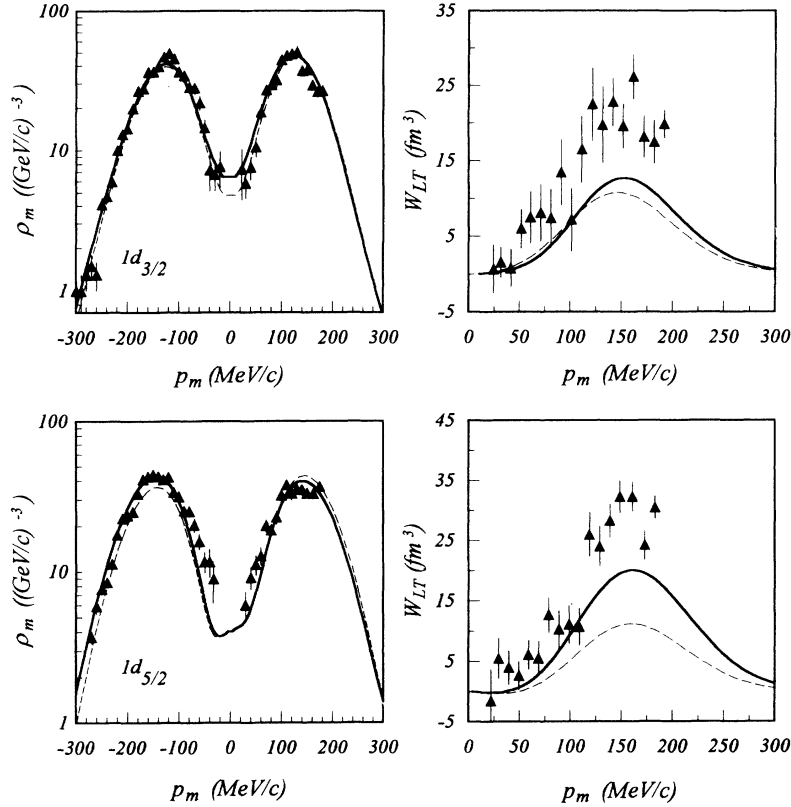


FIG. 11. Reduced cross sections and W_{LT} for $^{40}\text{Ca}(e, e'p)^{39}\text{K}(1d_{3/2}^{-1}; \text{g.s.})$ and $^{40}\text{Ca}(e, e'p)^{39}\text{K}(1d_{5/2}^{-1}; 5.26 \text{ MeV}, 5.60 \text{ MeV}, 6.36 \text{ MeV})$. (a) dashed line: DWIA, (b) full line: one- and two-body contributions in the nuclear current. An overall spectroscopic factor is used for the cross sections and the corresponding structure functions [$S(1d_{3/2})=0.48$, $S(1d_{5/2})=0.33$]. The data are from Refs. [13,14].

ditional measurable quantity W'_{LT} has as its main advantage that it vanishes identically in the plane wave impulse approximation (the escaping proton is described by a plane wave) [9]. So, the shape of the calculated W'_{LT} term is *completely determined* by the final-state interaction (FSI) and the different contributions in the nuclear current. In comparison with the results for the W_{LT} term, we observe a similar spin-dependent behavior with respect to the two-body nuclear current. For both single-particle orbits, the shape remains almost unaffected compared to the DWIA calculation. Whereas a small quenching is observed for the $1p_{1/2}$ state, pionic contributions seem to enhance the fifth structure function for the $1p_{3/2}$ state. Generally, the effect of the two-body contributions is more apparent in the W_{LT} term than in the corresponding W'_{LT} structure function.

Until now, all conclusions drawn referred to ^{16}O results. Similar calculations have been performed for virtual photon induced proton ejection from the target nucleus ^{40}Ca . We have calculated cross sections and structure functions for the spin-orbit partners $1d_{3/2}$ and $1d_{5/2}$. The results for the reduced cross sections and interference structure functions W_{LT} are displayed in Fig. 11. Once again, meson contributions in the current are not negligible and can account for part of the discrepancy between the IA calculations and the data. Due to the spin-dependent behavior of the Δ current, the W_{LT} function for the $1d_{3/2}$ state and the $1d_{5/2}$ state is modified in a different way. This conclusion is in total conformity with the results for the spin-orbit partners $1p_{1/2}$ and $1p_{3/2}$ in ^{16}O .

IV. CONCLUSIONS

The results presented here indicate the importance of two-body contributions in the nuclear current in order to reach a complete description of the $(\vec{e}, e'p)$ cross section and structure functions under quasifree conditions. Whereas the gross features of the cross section can be understood in a one-body picture, this model fails to describe the total cross section and the separated structure functions simultaneously. Going beyond the impulse approximation, we have accounted for two-body contributions in the current related to one-pion exchange and intermediate $\Delta(1232)$ creation. Calculations were performed for proton knockout from the target nuclei ^{16}O and ^{40}Ca . The results were shown to be rather insensitive to the model assumptions with respect to the pion and hadronic form factor. The charge-current interference structure function W_{LT} is found to be strongly affected by the two-body currents. A reasonable agreement with the data could be obtained within a model that accounts for the FSI within an HF-RPA model and in which one and two-body photoabsorption mechanisms are included. Coulomb distortion effects have been calculated in the CDWIA formalism. For the nuclei under consideration, the distortions in the electron waves are found to be rather marginal. Rather than the cross section the separated structure functions are sensitive to the different aspects of the reaction mechanism. In this sense, a further exploration of the separate structure functions opens good perspectives to obtain a better insight into the nature of the $(e, e'p)$ reaction mechanism.

ACKNOWLEDGMENTS

The authors are grateful to K. Heyde for fruitful discussions and suggestions. This work has been supported

by the Inter-University Institute for Nuclear Sciences (IIKW) and the National Fund for Scientific Research (NFWO).

-
- [1] S. Frullani and J. Mougey, *Adv. Nucl. Phys.* **14**, 1 (1984).
 [2] Y. Jin, K. Zhang, D. S. Onley, and L. E. Wright, *Phys. Rev. C* **47**, 2024 (1993).
 [3] A. Picklesimer, J. W. Van Orden, and S. J. Wallace, *Phys. Rev. C* **32**, 1312 (1985).
 [4] S. Boffi, C. Giusti, and F. D. Pacati, *Phys. Rep.* **226**, 1 (1993).
 [5] J. Ryckebusch, K. Heyde, D. Van Neck, and M. Waroquier, *Phys. Lett. B* **216**, 252 (1988).
 [6] M. Bernheim *et al.*, *Nucl. Phys.* **A375**, 381 (1982).
 [7] J. Ryckebusch, M. Waroquier, K. Heyde, J. Moreau, and D. Ryckbosch, *Nucl. Phys.* **A476**, 237 (1988).
 [8] M. Cavinato, M. Marangoni, and A. M. Saruis, *Z. Phys. A* **335**, 401 (1990).
 [9] A. S. Raskin and T. W. Donnelly, *Ann. Phys.* **191**, 78 (1989).
 [10] A. Picklesimer and J. W. Van Orden, *Phys. Rev. C* **40**, 290 (1989).
 [11] L. Chinitz *et al.*, *Phys. Rev. Lett.* **67**, 568 (1991).
 [12] C. M. Spaltro, H. P. Blok, E. Jans, L. Lapikás, M. van der Schaar, G. van der Steenhoven, and P. K. A. de Witt Huberts, *Phys. Rev. C* **48**, 2385 (1993).
 [13] L. Lapikás, *Nucl. Phys.* **A553**, 297c (1993).
 [14] H. Blok, private communication.
 [15] M. Waroquier, J. Ryckebusch, J. Moreau, K. Heyde, N. Blasi, S. Y. van der Werf, and G. Wenes, *Phys. Rep.* **148**, 249 (1987).
 [16] D. O. Riska, *Phys. Rep.* **181**, 207 (1989).
 [17] S. Galster, H. Klein, J. Moritz, K. H. Schmidt, D. Wegener, and J. Bleckwenn, *Nucl. Phys.* **B32**, 221 (1971).
 [18] T. Ericson and W. Weise, *Pions and Nuclei* (Oxford Science Publications, Oxford, 1988).
 [19] T. deForest and J. D. Walecka, *Adv. Phys.* **15**, 1 (1966).
 [20] J. Ryckebusch, L. Macheuil, M. Vanderhaeghen, and M. Waroquier, *Nucl. Phys.* **A568**, 828 (1994).
 [21] V. Van der Sluys, J. Ryckebusch, M. Waroquier, in preparation.
 [22] H. Überall, *Electron Scattering from Complex Nuclei* (Academic Press, London, 1971).
 [23] Y. Yin, D. S. Onley, and L. E. Wright, *Phys. Rev. C* **45**, 1311 (1992).
 [24] T. D. DeForest, Jr., *Nucl. Phys.* **A392**, 232 (1983).
 [25] R. Machleidt, K. Holinde, and Ch. Elster, *Phys. Rep.* **149**, 1 (1987).
 [26] T. Sasakawa, S. Ishikawa, Y. Wu, and T-Y. Saito, *Phys. Rev. Lett.* **68**, 3503 (1992).
 [27] C. Papanicolas, in *Proceedings of the 6th Workshop on Perspectives in Nuclear Physics at Intermediate Energies*, Trieste 1993, edited by S. Boffi, C. Ciofi degli Atti, and M. M. Giannini (World Scientific, Singapore, to be published).